CORNELL UNIVERSITY MATHEMATICS DEPARTMENT SENIOR THESIS

Topological Entropy Bounds for Hyperbolic Dynamical Systems

A THESIS PRESENTED IN PARTIAL FULFILLMENT
OF CRITERIA FOR HONORS IN MATHEMATICS

Rafael Mariano Frongillo

May 2007

BACHELOR OF ARTS, CORNELL UNIVERSITY

THESIS ADVISOR(S)

John Smillie
Department of Mathematics

Topological Entropy Bounds for Hyperbolic Dynamical Systems

Rafael M. Frongillo*

May 2, 2007

Abstract

We describe an automated method for computing rigorous lower bounds for topological entropy which was originally introduced in [DFTn07]. We combine this method with the work of Zin Arai in [Araar] to find rigorous lower bounds on topological entropy for 43 hyperbolic plateaus of the Hénon map.

1 Introduction

In the field of Dynamical Systems, computers are most often used as tools for exploration; computer iteration of maps can give fairly good impressions of the true underlying dynamics. Due to round-off errors, however, these impressions are sometimes misleading. We present a method which, although automated, yields rigorous results. Specifically, our method establishes the existence of a certain amount of chaos for a particular dynamical system, with topological entropy as a measure of chaos.

We apply this technique to the Hénon family of maps. There are several reasons for this choice. First, the Hénon maps are considered a standard place to test new ideas in dynamical systems. Secondly, we seek to expand upon work done by Zin Arai [Araar] and Davis, Mackay, and Sannami [DMS91] on the Hénon maps.

The Hénon maps were originally proposed by Hénon because of evidence of a strange attractor for the classical parameter values $a = 1.4$ and $b = 0.3$. We study these parameters in [DFTn07]. In this paper, we look at parameters for which the Hénon maps exhibit different behavior; namely, we focus on the parameters for which the maps are uniformly hyperbolic.

In this setting, we combine our results regarding lower bounds for topological entropy with the results of Zin Arai, where he computes hyperbolic plateaus, to obtain a global view of entropy as a function of the parameters. Furthermore, we compare our rigorous results to the conjectures given by Davis, Mackay, and Sannami.

*Cornell University

2 Background

2.1 Symbolic Dynamics

Symbolic dynamics is a useful tool for understanding complicated dynamical systems. In particular, we focus on subshifts of finite type, which is introduced below in Definition 2.4. This system is easily analyzed, and for this reason we try to show a relationship between our particular dynamical system of interest and a subshift, so that we can gain useful insights about the behavior of our original system. Symbolic dynamics is a fascinating field with many other applications besides the one we exploit; for a much more detailed introduction to symbolic dynamics, see [LM95].

Definition 2.1 (Directed graph). *The pair $G = (V, E)$ is called a* directed graph*, where V denotes the vertex set, and $E \subseteq V \times V$ denotes the edge set.*

Definition 2.2 (Transition matrix). *Let $G = (V, E)$ be a directed graph with $V = \{v_1, \ldots, v_n\}$. The* transition matrix *for G is the $n \times n$ matrix A with $A_{ji} = 1 \iff (v_i, v_j) \in E$.*

This matrix is usually called an adjacency matrix in graph theory (see e.g. [Eve79] or [LM95]), and often has $A_{ij} = 1$ when $(i, j) \in E$. We adopt the reverse convention so that the image, or outgoing neighbors, of a vertex i in G is the same as the nonzero entries of $A\vec{e}_i$.

Definition 2.3 (Graph full trajectory). *A* full trajectory *of a graph $G = (V, E)$ is a sequence $\gamma = \ldots, v_{-1}, v_0, v_1, \ldots$ such that $(v_i, v_{i+1}) \in E$ for all $i \in \mathbb{Z}$.*

Definition 2.4 (Subshift of finite type). *Let $G = (V, E)$ be a directed graph. Then the* symbol space *X_G is the set of all full trajectories of G. The corresponding* symbol map *$\sigma_G : X_G \to X_G$ is defined as*

$$\sigma_G\big((s_k)_{k\in\mathbb{Z}}\big) := (s_{k+1})_{k\in\mathbb{Z}}. \tag{1}$$

The pair (X_g, σ_G) is called a subshift of finite type*.*

In graph-theoretical terms, X_G is the set of bi-infinite walks on G. The map σ_G just shifts these sequences by 1. The term "subshift of finite type" refers to the fact that G only allows a subset X_G of the *full shift* corresponding to the directed complete graph on n vertices, and that we have only finitely many symbols. For a suitable metric d on X_G, we have that σ_G is a continuous map; for example, one could take

$$d\big((s_k)_{k\in\mathbb{Z}}, (t_k)_{k\in\mathbb{Z}}\big) = \sum_{k=-\infty}^{\infty} \frac{|s_k - t_k|}{2^{|k|}}. \tag{2}$$

Under such a metric, (X_G, σ_G) is a continuous dynamical system.

We want to study invariant behavior of dynamical systems, so the following two definitions are useful.

Definition 2.5 (Strongly-connected component). *Given a graph $G = (V, E)$, define a relation $\leq_G$ on V, where $v \leq_G w$ if there is a (directed) path in G from v to w. Then the relation $=_G$, where $v =_G w \iff v \leq_G w$ and $w \leq_G v$ is an equivalence relation on V; a* strongly-connected component *of G is an equivalence class of $=_G$.*

In other words, a strongly-connected component is a set S of vertices such that for any two vertices v, w in S, there is a directed cycle in G going through v and w. In this way, strongly-connected components are "invariant", since they are necessarily cyclic.

Definition 2.6 (Graph invariant set). *The* invarant set *of the graph G is*

$$Inv(G) = \{v_i \mid \exists \text{ full trajectory } \gamma \text{ with } v_i \in \gamma\}. \tag{3}$$

In fact, it is easy to see that if $H = \mathrm{Inv}(G)$, then $X_G = X_H$. Thus, the subshifts (X_G, σ_G) and (X_H, σ_H) are the same. We will see later (Proposition 4.1) that the invariant set of G is closely related to the strongly-connect components of G.

2.2 Topological Entropy and Conjugacy

We use topological entropy to measure the relative complexity of different dynamical systems. If the topological entropy of a dynamical system f, denoted $h(f)$, is positive, we say that f is *chaotic*. Similarly, if $h(f) > h(g)$, then we say that f is more chaotic than g. Below is the formal definition of topological entropy.

Definition 2.7 (Topological entropy). *Let $f : X \to X$ be a continuous map with respect to a metric d. We say that a set $W \subseteq X$ is (n, ε)-separated under f if for any distinct $x, y \in W$ we have $d\big(f^j(x),\ f^j(y)\big) > \varepsilon$ for some $0 \leq j < n$. The* topological entropy *of f is*

$$h(f) := \lim_{\varepsilon \to \infty} \limsup_{n \to \infty} \frac{log(s_f(n, \varepsilon))}{n}, \tag{4}$$

where $s_f(n, \varepsilon)$ denotes the maximum cardinality of an (n, ε)-separated set under f.

The following is a more intuitive way of looking at topological entropy. Call a sequence $x, f(x), f^2(x), \ldots, f^{n-1}(x)$ an n-trajectory of f (the first n iterates of x). Call two points x, y ε-distinguishable if $d(x, y) > \varepsilon$; then $s_f(n, \varepsilon)$ is the maximum number of ε-distinguishable n-trajectories, where two trajectories are ε-distinguishable if some corresponding pair of points in the trajectories are. With this different interpretation, we can view $h(f)$ as measuring the exponential growth rate of the number of distinguishable n-trajectories under f.

While topological entropy can be difficult to calculate in general, there is a nice formula for subshifts of finite type which is given in the following theorem. For a proof, see [LM95] or [Rob95].

Theorem 2.8 (Topological entropy of a subshift). *Let G be a directed graph with transition matrix A, and let (X_G, σ_G) be the corresponding subshift of finite type. Then the topological entropy of σ_G is $h(\sigma_G) = \log(sp(A))$, where $sp(A)$ denotes the spectral radius (maximum magnitude of an eigenvalue) of A.*

To find lower bounds for topological entropy of a given f, our technique is to find a subshift of finite type which captures some of the complicated dynamics of f, and then take the easily-computable topological entropy of the subshift as a lower bound. Formally, we need to find a semi-conjugacy from f to the subshift:

Definition 2.9 (Conjugacy, semi-conjugacy). *Let $f : X \to X$ and $g : Y \to Y$ be continuous maps. A* conjugacy *from f to g is a bijective function $\phi : X \to Y$ such that $\phi \circ f = g \circ \phi$. A* semi-conjugacy *is the same except that ϕ need only be surjective.*

A usual candidate for a semi-conjugacy is the *itinerary function*, defined below.

Definition 2.10 (Itinerary function). *Assume $f : X \to X$ is invertible, and let $N \subseteq X$ be the union of disjoint compact sets $N_1, \ldots, N_k$. The* itinerary *of a point $x \in N$, if it exists, is the sequence $s^x := \ldots, s_{-1}, s_0, s_1, \ldots$ such that $f^n(x) \in N_{s_n}$ for all $n \in \mathbb{Z}$. Let $S = \{x \in N \mid s^x \text{ exists}\}$ and let G be a graph on vertices $\{1, \ldots, k\}$ such that s^x is a bi-infinite path in G for every $x \in S$. Then we define the* itinerary function *$\rho : S \to X_G$, by $\rho(x) = s^x$.*

We will see in Section 2.4 that the set S used above is called the maximal invariant set of N.

The reason that ρ is a good candidate for a semi-conjugacy is that it already satisfies $\rho \circ f = \sigma_G \circ \rho$, as one can easily check. To show that ρ is a semi-conjugacy, one only needs to show that ρ is surjective; we discuss one way to prove this in Section 4.3.

If we can somehow prove the existence of a semi-conjugacy, which could be the itinerary map ρ discussed above, then the entropy of the subshift is a lower bound for the entropy of f. This is a consequence of the following theorem (see Chapter 8 of [Rob95] for a proof).

Theorem 2.11 (Topological entropy and semi-conjugacy). *Let f and g be continuous maps, and let ϕ be a semi-conjugacy from f to g. Then $h(f) \geq h(g)$.*

Note that if f and g are conjugate, theorem 2.11 applied twice gives us $h(f) = h(g)$. In other words, topological entropy is invariant under conjugacy; this coincides with the intuition that topological entropy is of a measure of chaos.

2.3 Shift Equivalence

The concept of shift equivalence comes up both in the definition of the Conley index in the next section, and in relation to symbolic dynamics (see Theorem 2.15). The general idea behind shift equivalence is to capture the eventual

behavior of a dynamical system, or the eventual range of a matrix. That is, two maps are shift equivalent roughly when high iterates of the maps behave in the same way. In particular, it ignores "transient" behavior.

The first type of shift equivalence, called *elementary shift equivalence*, is the strongest. A chain of such equivalence leads to a *strong shift equivalence*. Both of these are defined below.

Definition 2.12 (Elementary shift equivalence). *Let A and B be matrices. An* elementary shift equivalence *between A and B is a pair (R, S) such that*

$$A = RS \text{ and } B = SR. \tag{5}$$

In this case, we write $(R, S) : A \approx B$.

Definition 2.13 (Strong shift equivalence). *Two matrices A and B are* strongly shift equivalent with lag ℓ *if there exists a sequence of matrix pairs $(R_1, S_1), \ldots, (R_\ell, S_\ell)$ such that*

$$A = R_1S_1, \;\; S_1R_1 = R_2S_2, \;\; \ldots, \;\; S_{\ell-1}R_{\ell-1} = R_\ell S_\ell, \;\; S_\ell R_\ell = B. \tag{6}$$

In other words, for some $A = A_1, A_2, \ldots, A_{\ell-1}, A_{\ell+1} = B$ such that $(R_k, S_k) : A_k \approx A_{k+1}$ for all $k \leq \ell$. In this case we say that $\{(R_k, S_k)\}$ is a strong shift equivalence *between A and B, and we write $A \approx B$ (lag ℓ).*

While we will see in Theorem 2.15 that strong shift equivalence is the right notion for subshifts of finite type, the Conley index uses a more computable equvalence relation, called *weak shift equivalence*, or simply *shift equivalence*.

Definition 2.14 (Shift equivalence). *Two matrices A and B are* shift equivalent with lag ℓ *if there exist matrices R, S such that the following four conditions hold*

$$A^\ell = RS, \qquad B^\ell = SR, \tag{7}$$

$$AR = RB, \qquad SA = BS \tag{8}$$

In this case, we write $(R, S) : A \sim_\ell B$.

Shift equivalence is weak in the sense that $A \approx_\ell B \implies A \sim_\ell B$; see [LM95] for a proof. Note that this definition applies to group homomorphisms as well, and is an equivalence relation in that setting as well. In fact, we define the Conley index using shift equivalence in that setting. In the context of matrices, there is an important result due to R. F. Williams relating shift equivalence to symbolic dynamics [Wil73].

Theorem 2.15 (Shift equivalence and conjugacy). *For directed graphs G and H, the corresponding subshifts (X_G, σ_G) and (X_H, σ_H) are conjugate if and only if $G \approx H$ (G is strongly shift equivalent to H).*

This theorem allows us to prove that two subshifts are conjugate by a chain of simple matrix computations. Finding matrices that give a strong shift equivalence, however, can be a very difficult problem. In Section 3, we discuss a variant of this problem, namely finding a smaller matrix B in the same strong shift equivalence class as A.

2.4 Conley Index

The Conley index is a topological generalization of Morse theory which allows us to study our dynamical system $f : X \to X$ with the computer, where numerical errors are necessarily present. Because of its topological nature, the Conley index is robust with respect to small numerical errors in the computation, but still provides enough information about f to be useful. To begin, we introduce the invariant set, which is the main object in Conley index theory.

Definition 2.16 (Maximal invariant set). *The* maximal invariant set *of a set $A \subseteq X$, written $Inv(A, f)$, is the largest set $S \subseteq A$ such that $f(S) = S$.*

The robustness of the Conley index comes primarily from the notion of isolation, defined below. This property ensures that small enough perturbations will not effect the result.

Definition 2.17 (Isolating neighborhood, isolated invariant set). *A set N is an* isolating neighborhood *of a set I if*

$$I = Inv(N, f) \subseteq Int\ (N), \tag{9}$$

where $Int\ (N)$ denotes the interior of N. The set I is called an isolated invariant set *relative to N.*

Below are the remaining definitions needed for the Conley index.

Definition 2.18 (Index pair, Index map). *A pair (P_1, P_0) of compact sets, $P_0 \subseteq P_1 \subseteq X$, is an* index pair *for $I \subseteq X$ if*

1. *The* index map $f_P : (P_1/P_0, [P_0]) \to (P_1/P_0, [P_0])$ *for P defined by*

$$f_P([x]) := \begin{cases} f(x) & \text{if } f(x) \in P_1 \\ [P_0] & \text{otherwise} \end{cases} \tag{10}$$

   is continuous,

2. *The closure of $P_1 \setminus P_0$ is an isolating neighborhood for I.*

Definition 2.19 (Homology Conley index). *Let I be an isolated invariant set, and let $P = (P_1, P_0)$ be an index pair for I, with index map f_P. The* Conley index *of I is the shift equivalence class of the map f_{P*}:*

$$Con(I) := [f_{P*}]_\sigma, \tag{11}$$

where $f_{P*} : H_*(P_1, P_0) \to H_*(P_1, P_0)$ is the map f_P induces on the relative homology groups $H_*(P_1, P_0)$.

A crucial result is that the Conley index is well-defined [MM02], meaning that the shift equivalence class of f_{P*} is the same for all index pairs P of a particular isolated invariant set I. The real power of the Conley index becomes more clear with the introduction of a quantity called the *Lefschetz number*. In the subsequent theorem, this number puts the topological information encoded in the Conley index to good use.

Definition 2.20 (Lefschetz number). *Let S be an isolated invariant set and let $P = (P_1, P_0)$ be an index pair for S. The* Lefschetz number *of S is defined as*

$$L(S, f) := \sum_k (-1)^k \operatorname{tr} f_{P\,k} \tag{12}$$

where and $\operatorname{tr} f_{P\,k}$ denotes the trace of the k-th homology map $f_{P\,k} : H_k(P_1, P_0) \to H_k(P_1, P_0)$.

Theorem 2.21 (Lefschetz fixed point theorem). *If S is an isolated invariant set and $L(S, f) \neq 0$, then S contains a fixed point.*

For a proof of the Lefschetz fixed point theorem, see [Szy97]. We will use a corollary to this theorem to show the existence of periodic orbits in Section 4.3 (Corollary 4.2).

We wish to automate the computation of the Conley index and Lefschetz numbers, so at some point we need to feed the map to a computer. The following sets the stage for how this is done, starting from the discretezation of the phase space into n-dimensional boxes, to how to define f on these boxes, and finally how to use Conley index theory in this discrete setting.

Definition 2.22 (Grid in phase space, topological realization). *Given $X \subseteq W \subseteq \mathbb{R}^n$ such that $W = [a_1, b_1] \times \cdots \times [a_n, b_n]$, we define a* grid $\mathcal{G}^{(r)}$ *at* resolution r *to be the set*

$$\mathcal{G}^{(r)} = \left\{ \prod_{i=1}^{n} [x_i,\ x_i + d_i] \,\middle|\, \frac{x_i - a_i}{d_i} \in \{0, \ldots, 2^r - 1\} \right\}, \tag{13}$$

where $d_i = (b_i - a_i)/2^r$. We will refer to the elements of $\mathcal{G}^{(r)}$ as boxes. *The* topological realization *of a set $\mathcal{B}$ of boxes is defined as*

$$|\mathcal{B}| := \bigcup_{B \in \mathcal{B}} B \tag{14}$$

We now develop a notion of the dynamics on the boxes induced by f. Moreover, as we wish to do rigorous computations, we need to keep track of any errors that arise in the computation. The following framework allows us to do that.

Definition 2.23 (Multivalued map). *Let Y be the powerset of X. A function $F : X \to Y$ is a* multivalued map *on X, so that $F(x) \subseteq X$ for all x. We denote this as $F : X \rightrightarrows X$. When X is discrete we sometimes think of F as a directed graph.*

Definition 2.24 (Enclosure, continuous selector). *Let $F : X \rightrightarrows X$. A* continuous selector *for F is a continuous map $f : X \to X$ such that for all $x \in X$, $f(x) \in F(x)$ and $F(x)$ is homotopic to a point. In this case, F is an* enclosure *of f.*

Definition 2.25 (Grid enclosure). *Given a grid $\mathcal{G}$ and a map $f : X \to X$, a* grid enclosure *of f is a multivalued map $\mathcal{F} : \mathcal{G} \rightrightarrows \mathcal{G}$ such that the map $|\mathcal{F}| \colon X \rightrightarrows X$ defined by*

$$|\mathcal{F}|(x) := |\mathcal{F}(\{B \mid x \in B\})| \tag{15}$$

is an enclosure of f.

In this terminology, we want to find a grid enclosure $\mathcal{F}$ of f. We obtain $\mathcal{F}$ using interval arithmetic, to ensure that for any box B, its image $\mathcal{F}(B)$ contains $f(x)$ for all $x \in B$.

We next define the Conley index in the setting of a discrete space, so that we can make rigorous statements about the dynamics of f. As above, we first define an analogous isolated invaliant set and isolating neighborhood.

Definition 2.26 (Box isolating neighborhood, box invariant set). *A* grid neighborhood *$o(\mathcal{S})$ of $\mathcal{S}$ is the set*

$$o(\mathcal{S}) = \{B \in \mathcal{G} \mid \ |B| \cap |\mathcal{S}| \neq \emptyset\}. \tag{16}$$

A set $\mathcal{I}$ is a box invariant set *relative to a set $\mathcal{N}$ if*

$$\mathcal{I} = Inv(\mathcal{N}, \mathcal{F}) := Inv(\mathcal{F}|_{\mathcal{N}}), \tag{17}$$

where $Inv(\mathcal{F}|_{\mathcal{N}})$ is the invariant set of the directed graph associated to $\mathcal{F}$, restricted to $\mathcal{N}$ (see Definition 2.6). If in addition we have $o(\mathcal{I}) \subseteq \mathcal{N}$, then $\mathcal{N}$ is a box isolating neighborhood *of $\mathcal{I}$.*

Note that if $\mathcal{F}$ is a grid enclosure, then $|\mathcal{N}|$ is an isolating neighborhood of $\mathrm{Inv}(|\mathcal{I}|, f)$. This leads to the following definition.

Definition 2.27 (Box index pair). *A pair $\mathcal{P} = (\mathcal{P}_1, \mathcal{P}_0)$ of box sets is a* box index pair *for a grid enclosure $\mathcal{F}$ if the corresponding topological realization $|\mathcal{P}| = (|P_1|, |\mathcal{P}_0|)$ is an index pair for any continuous selector $f \in |\mathcal{F}|$. That is, $\mathrm{cl}(P_1 \setminus P_0) = |\mathcal{P}_1 \setminus \mathcal{P}_0|$ is an isolating neighborhood under f and the quotient map f_P as in defined in Definition 2.18 is continuous.*

It is not obvious that box index pairs are easily computable. There is, however, an efficient algorithm to compute them, based on the fact that the topological realization of a grid isolating neighborhood is an isolating neighborhood, as mentioned above. This is given as Algorithm 2 in Section 4.2.

From a box index pair $\mathcal{P} = (\mathcal{P}_1, \mathcal{P}_0)$, we define its Conley index to be the Conley index of $|\mathcal{P}| = (|\mathcal{P}_1|, |\mathcal{P}_0|)$ as given in Definition 2.19. That is, the Conley index of $\mathcal{P}$ is the map on relative homology induced by $f_{|\mathcal{P}|}$.

3 Simplifying Shift Equivalence Representatives

The notion of shift equivalence shows up in two important places in the theory behind our approach; the first is in the definition of the Conley index, and the

second is in the theory of symbolic dynamics (see Theorem 2.15). In both of these most cases, we seek the simplest possible representative of the shift equivalence class of a given matrix. The task of finding the smallest representative can be difficult, the following two subsections discuss how one can at least simplify or reduce the given matrix to a smaller representative.

3.1 Reducing Subshifts

Given a subshift of finite type (X_G, σ_G) for a graph G, it is often of interest to know whether there is a graph H on fewer vertices such that (X_G, σ_G) and (X_H, σ_H) are conjugate. By Theorem 2.15, it is enough to prove that the transition matrices A and B for G and H, respectively, are strongly shift equivalent. We give a procedure for finding such a B below.

Let A be $n \times n$. We wish to find conditions that allow us to replace A with a smaller $n-1 \times n-1$ matrix B which is strongly shift equivalent to A. The following two conditions allow us to do exactly that by contracting vertices i and j.

$$\textbf{Forward Condition:} \quad A\vec{e}_i = A\vec{e}_j \text{ and } (\vec{e}_i^{\top} A) \cdot (\vec{e}_j^{\top} A) = 0 \tag{18}$$

$$\textbf{Backward Condition:} \quad (A\vec{e}_i) \cdot (A\vec{e}_j) \text{ and } \vec{e}_i^{\top} A = \vec{e}_j^{\top} A \tag{19}$$

Here $\vec{e}_i$ denotes the column vector with a 1 in position i and zeros elsewhere. The forward condition says that i and j have the same image but disjoint preimages, and the backward condition says they have the same preimage but disjoint images. Note that the backward condition is the same as the forward condition for i and j in $A^{\top}$. The following result allows us to reduce A to B if either of these conditions are satisfied for some pair of vertices. A somewhat different proof involving graph splittings is given in chapter 2 of [LM95].

Theorem 3.1 (Strong Shift Equivalence by Contraction). *If i and j satisfy the forward condition (18) or backward condition (19) for an $n \times n$ transition matrix A, then A is strongly shift equivalent to the $n-1 \times n-1$ matrix B obtained by contracting vertices i and j to i in A. Specifically, if the forward condition is satisfied, then $B = YAX$, where*

$$X = \left[\begin{array}{c|c} I_{j-1} & 0 \\ \hline \vec{0} & \vec{0} \\ \hline 0 & I_{n-j} \end{array}\right], \quad Y = \left[\begin{array}{c|c|c} I_{j-1} & \vec{e}_i & 0 \\ \hline 0 & \vec{0} & I_{n-j} \end{array}\right], \tag{20}$$

and X and Y are $n \times n-1$ and $n-1 \times n$ matrices, respectively. If the backward condition is satisfied, then $B = X^{\top} A Y^{\top}$ for the same X and Y.

Proof. Assume the forward condition is satisfied for i and j in A. By direct computation, we have

$$XY = \left[\begin{array}{c|c} I_{j-1} & 0 \\ \hline \vec{0} & \vec{0} \\ \hline 0 & I_{n-j} \end{array}\right] \left[\begin{array}{c|c|c} I_{j-1} & \vec{e}_i & 0 \\ \hline 0 & \vec{0} & I_{n-j} \end{array}\right] = \left[\begin{array}{c|c|c} I_{j-1} & \vec{e}_i & 0 \\ \hline \vec{0} & 0 & \vec{0} \\ \hline 0 & \vec{0} & I_{n-j} \end{array}\right], \tag{21}$$

and thus $AXY\vec{e}_k = A\vec{e}_k$ if $k \neq j$ and $AXY\vec{e}_j = A\vec{e}_i$. By the forward condition (18) we have $A\vec{e}_j = A\vec{e}_i$, so in fact $AXY = A$. Letting $R = AX$ and $S = Y$, we now have

$$RS = (AX)Y = A \tag{22}$$
$$SR = Y(AX) = B. \tag{23}$$

Thus, $(R, S) : A \approx B$.

If instead the backward condition is satisfied, then i and j satisfy the forward condition for $A^\top$ by the remark above. Thus, $A^\top XY = A^\top$ by the above computation. Now take $R = Y^\top$ and $S = X^\top A$; then

$$RS = Y^\top(X^\top A) = (A^\top XY)^\top = (A^\top)^\top = A \tag{24}$$
$$SR = (X^\top A)Y^\top = B, \tag{25}$$

so again $(R, S) : A \approx B$. □

By applying Theorem 3.1 repeatedly, as long as there exist i, j satisfying either contraction condition, we can reduce A to a much smaller representative of its strong shift equivalence class; the resulting matrix B at the end of this process corresponds to a subshift (X_H, σ_H) which is therefore conjugate to (X_G, σ_G). In general, however, there are many pairs (i, j) to choose from, and finding the sequence of contractions that leads to the smallest possible representative is roughly equivalent to searching all possible partitions of $\{1, \ldots, n\}$, of which there are exponentially many in n.

3.2 Reducing Matrices over $\mathbb{Z}$

To prove that the itinerary function defined in Definition 2.10 is surjective, we use the Lefschetz theorem, which involves computations with the index map f_{P*}. As we will see in section 4.3, the fewer generators we have in each region of the phase space, the easier the computations are. For this reason, we try to find the smallest representative of the shift equivalence class of f_{P*} before doing these computation. This simplification corresponds to ignoring the transient generators, which are generators not in the image or preimage of a high enough iterate of f_{P*}.

The following theorem, which is a general result on the shift equivalence of matrices over $\mathbb{R}$, will give us our desired representative.

Theorem 3.2. *Let*

$$A = \begin{bmatrix} A_{11} & 0 & 0 \\ A_{21} & A_{22} & 0 \\ A_{31} & A_{32} & A_{33} \end{bmatrix} \in \mathbb{R}^{n \times n}$$

be a 3×3 *block lower-triangular matrix, with square matrices* A_{ii} *on the diagonal. If* $A_{11}^k = 0$ *and* $A_{33}^k = 0$ *for some* k*, then* A *is shift equivalent to* A_{22} *with lag* $\ell = 2k$*.*

Proof. For $i = 1, 2, 3$, let $n_i \times n_i$ be the size of the square matrix A_{ii}, and define projection and inclusion maps respectively as follows:

$$\pi = \begin{bmatrix} 0_{n_{22} \times n_{11}} & I_{n_{22}} & 0_{n_{22} \times n_{33}} \end{bmatrix}, \qquad \iota = \pi^\top. \tag{26}$$

We will show that the matrices $R = \pi A^k$ and $S = A^k \iota$ give the desired shift equivalence between A and A_{22}.

Let $(A^n)_{ij}$ denote the $n_i \times n_j$ block of A^n. Then

$$A^n = \begin{bmatrix} (A_{11})^n & 0 & 0 \\ (A^n)_{21} & (A_{22})^n & 0 \\ (A^n)_{31} & (A^n)_{32} & (A_{33})^n \end{bmatrix}, \tag{27}$$

and by induction on n,

$$\begin{aligned} (A^n)_{21} &= \sum_{i=1}^{n} A_{22}^{i-1} A_{21} A_{11}^{n-i} \\ (A^n)_{32} &= \sum_{i=1}^{n} A_{33}^{i-1} A_{32} A_{22}^{n-i}. \end{aligned} \tag{28}$$

In this notation, we also have that

$$R = \begin{bmatrix} (A^k)_{21} & A_{22}^k & 0 \end{bmatrix}, \quad S = \begin{bmatrix} 0 \\ A_{22}^k \\ (A^k)_{32} \end{bmatrix}.$$

We now verify the conditions of shift equivalence.

Condition 1: $A_{22}R = RA$

We have

$$A_{22}R = \begin{bmatrix} A_{22}(A^k)_{21} & (A_{22})^{k+1} & 0 \end{bmatrix}$$

and

$$RA = \begin{bmatrix} (A^k)_{21}A_{11} + (A_{22})^k A_{21} & (A_{22})^{k+1} & 0 \end{bmatrix}$$

so it suffices to show that the first block entries are equal. Using (28) and the

fact that $A_{11}^k = 0$,

$$\begin{aligned} A_{22}(A^k)_{21} &= \sum_{i=1}^{k} A_{22}^i A_{21} A_{11}^{k-i} \\ &= \sum_{l=2}^{k+1} A_{22}^{l-1} A_{21} A_{11}^{k+1-l} \\ &= \sum_{l=1}^{k+1} A_{22}^{l-1} A_{21} A_{11}^{k+1-l} \\ &= \sum_{l=1}^{k} A_{22}^{l-1} A_{21} A_{11}^{k+1-l} + A_{22}^k A_{21} \\ &= (A^k)_{21} A_{11} + A_{22}^k A_{21} \end{aligned}$$

Condition 2: $AS = SA_{22}$
Follows similarly to the verification of Condition 1.

Condition 3. $RS = (A_{22})^{2k}$
This follows from a simple computation:

$$RS = \begin{bmatrix} (A^k)_{21} & (A_{22})^k & 0 \end{bmatrix} \begin{bmatrix} 0 \\ (A_{22})^k \\ (A^k)_{32} \end{bmatrix} = (A_{22})^{2k}.$$

Condition 4. $SR = A^{2k}$
By (27), and the fact that $A_{11}^k = 0 = A_{33}^k$, we have

$$A^{2k} = (A^k)^2 = \begin{bmatrix} 0 & 0 & 0 \\ (A^k)_{21} & A_{22}^k & 0 \\ (A^k)_{31} & (A^k)_{32} & 0 \end{bmatrix}^2 = \begin{bmatrix} 0 & 0 & 0 \\ A_{22}^k (A^k)_{21} & A_{22}^{2k} & 0 \\ (A^k)_{32}(A^k)_{21} & (A^k)_{32} A_{22}^k & 0 \end{bmatrix}.$$

On the other hand,

$$SR = \begin{bmatrix} 0 \\ A_{22}^k \\ (A^k)_{32} \end{bmatrix} \begin{bmatrix} (A^k)_{21} & A_{22}^k & 0 \end{bmatrix} = \begin{bmatrix} 0 & 0 & 0 \\ A_{22}^k (A^k)_{21} & A_{22}^{2k} & 0 \\ (A^k)_{32}(A^k)_{21} & (A^k)_{32} A_{22}^k & 0 \end{bmatrix}.$$

Thus, we have verified the conditions and A is shift equivalent to A_{22}. □

We will show in Section 4.2 that, by a reordering of basis elements, f_{P*} satisfies the hypotheses for Theorem 3.2.

4 Automated Method for Rigorous Lower Bounds

4.1 Overview

Our overall goal is to find a semi-conjugacy from our original dynamical system f to a subshift of finite type (X_G, σ_G). This semi-conjugacy will give us a lower bound on the topological entropy of f.

The procedure we use begins by discretizing the phase space X by computing a grid $\mathcal{G}^{(r)}$ for some resolution r, and then computing the multivalued map $\mathcal{F}$ on boxes. We do this using a software package called GAIO (Global Analysis of Invariant Objects) which is maintained by Oliver Junge [DFJ01], and an interval arithmetic package called INTLAB [Cse99]. From $\mathcal{G}$ and $\mathcal{F}$ we compute a lower bound for the topological entropy of f in three phases:

I Find a box collection $\mathcal{S}$ that captures as much of the complicated dynamics of f as possible.

II Compute an isolated invariant set from S and compute its index pair and index map.

III Find a directed graph whose corresponding subshift can be proven to be semi-conjugate to f via the Lefschetz fixed point theorem.

The following two subsections discuss the last two phases, which correspond to the bulk of the automated proof. The first phase is discussed last, as there are many different methods for producing a good box collection.

4.2 Phase II: Obtaining the Index Map

The second phase of the computation takes the box set $\mathcal{S}$ computed in Phase I, which hopefully captures some complicated dynamics from our dynamical system f, and computes the Conley index of an isolated invariant set $\mathcal{I}$ "grown" from $\mathcal{S}$.

The first step is computing an isolated invariant set $\mathcal{I}$ with isolating neighborhood $\mathcal{N}$ from the given box set $\mathcal{S}$. We do this by invoking the Algorithm 1.

$\mathcal{N} \leftarrow \mathcal{S}$
repeat
  $\mathcal{I} \leftarrow \mathrm{Inv}(P|_{\mathcal{N}})$
  $\mathcal{N}_0 \leftarrow \mathcal{N}$
  $\mathcal{N} \leftarrow o(\mathcal{I})$
until $\mathcal{N} \subseteq \mathcal{N}_0$

Algorithm 1: Grow isolated invariant set

Here P denotes the graph (or transition matrix) for $\mathcal{F}$ and $P_{\mathcal{S}}$ denotes the subgraph of P on the vertices of $\mathcal{S}$. The next task is to compute a box index pair $\mathcal{P} = (\mathcal{P}_1, \mathcal{P}_0)$ for $\mathcal{I}$. As we mentioned after Definition 2.27, there is also

an efficient algorithm for finding $\mathcal{P}$. Assuming $\mathcal{N}$ is a box isolating neighborhood isolating the box invariant set $\mathcal{I}$, as produced by Algorithm 1, we use the following algorithm.

$\mathcal{P}_0 \leftarrow \emptyset$
$\mathcal{K} \leftarrow \mathcal{F}(\mathcal{N}) \cap (o(\mathcal{N}) \setminus \mathcal{N})$
while $\mathcal{K} \neq \emptyset$ **do**
  $\mathcal{P}_0 \leftarrow \mathcal{P}_0 \cup \mathcal{K}$
  $\mathcal{K} \leftarrow (\mathcal{F}(\mathcal{P}_0) \cap o(\mathcal{N})) \setminus \mathcal{P}_0$
end while
$\mathcal{P}_1 \leftarrow \mathcal{N} \cup \mathcal{P}_0$

Algorithm 2: Build index pair

Let $P = (P_1, P_0) = |\mathcal{P}|$, which is the index pair for the isolated invariant set I in $|\mathcal{I}|$ (see the discussion at the end of Section 2.4 for this notation). We can now compute the map f_{P*} induced on relative homology groups by the index map f_P for (P_1, P_0) using a program called *homcubes* [Pil98]. This useful program is part of the CHomP package [cho], and does exactly what we need here.

Finally, once we have f_{P*}, we reduce it to a smaller representative of its shift equivalence class $[f_{P*}]_\sigma$. Note that since we are considering $f : X \to X$ with $X \subseteq \mathbb{R}^n$, and the box collections we are considering are all finite, the map $f_{Pk} : H_k(P_1, P_0) \to H_k(P_1, P_0)$ is linear on a finitely generated free abelian group. Since $H_k(P_1, P_0)$ and f_{Pk} must be trivial for $k > n$, we can think of f_{P*} as a finite list of matrices with integer entries.

With this matrix representation, we must show that by a change of basis, f_{P*} has a block lower-triangular form and satisfies the nilpotency conditions of Theorem 3.2. Since we can always satisfy these condition trivially by taking the blocks A_{11} and A_{33} to have size 0, the task becomes maximizing the size of these blocks, so the remaining middle block, the new representative, is as small as possible.

In practice, we consider the directed graph G_{P*} whose transitions are given by the nonzero entries of f_{P*}. We then merely compute the invariant set $\mathrm{Inv}(G_{P*})$ of G_{P*}, using depth-first search to find the strongly connected components (see Definition 2.5) and connections between them, and take the submatrix of f_{P*} corresponding to the elements of $\mathrm{Inv}(G_{P*})$ as the new representative. The following shows that this procedure is validated by Theorem 3.2.

Proposition 4.1 (Invariant set and strongly-connected components). *Let $G = (V, E)$ be a directed graph. Then Inv(G) is the set of vertices in strongly-connected components of G and those on paths between strongly-connected components. If G is connected, there is a partitioning $G_<$, Inv(G), $G_>$ of the vertices, such that the only directed edges between partitions are from $G_<$ to Inv(G) or $G_>$ and from Inv(G) to $G_>$.*

Proof. Define a relation $\leq_G$ on V as in Definition 2.5, and let S be the set of vertices in strongly-connected components or on paths between them.

(Inv$(G) \subseteq S$): Let $v \in \text{Inv}(G)$, and let $\gamma = \ldots, v_{-1}, v_=, v_1, \ldots$ be a full trajectory in G with $v_0 = v$. Then certainly $v_i \leq_G v_j$ when $i < j$. Since there are finitely many vertices, there are only finitely many equivalence classes for $=_G$. Thus, since γ is nondecreasing with respect to this relation, there is some large N for which $v_i =_G v_N$ and $v_{-i} =_G v_{-N}$ for all $i > N$. Since the equivalence classes of $=_G$ are the strongly-connected components, γ starts and ends in a strongly-connected component, so $v \in S$.

(Inv$(G) \supseteq S$) Let $v \in S$. Then there are vertices w, x in stongly-connected components such that $w \leq_G v \leq_G x$. By definition of the relation, we have paths p_{wv} from w to v and p_{vx} from v to x. By definition of strongly-connected, we can find paths (cycles) c_w from w to w and c_x from x to x. Thus, we have a full trajectory through v: $\ldots c_w c_w c_w p_{wv} p_{vx} c_x c_x c_x \ldots$, so $v \in \text{Inv}(G)$.

If G is connected, then we can define

$$G_> = \{v \notin \text{Inv}(G) \mid \exists x \in \text{Inv}(G) \text{ s.t. } v \geq_G x\} \tag{29}$$

$$G_< = V(G) - \text{Inv}(G) - G_>. \tag{30}$$

Clearly, this is a partition of the vertices; we need only show that there are no paths out of $G_>$ and no paths from Inv(G) to $G_<$. If there were nodes $v \in \text{Inv}(G)$ and $w \in G_<$ with $v \leq_G w$, then we have $w \in G_>$ by definition of $G_>$, which contradicts $w \in G_<$. If $u \in G_>$ and $u \leq_G w$, then for some $v' \in \text{Inv}(G)$ we would have $v' \leq_G u \leq_G w$, which again contradicts the definition of $G_>$. Finally, if $u \leq_G v$, then as $v' \leq_G u$ for some $v' \in \text{Inv}(G)$, u would be on a connecting path between two strongly-connected components, and thus in Inv(G). Therefore, the only paths between these partitions are from $G_<$ to Inv$(G) \cup G_>$ and from Inv(G) to $G_>$. □

Let A be the matrix given by reordering the generators so that $(G_{P*})_<$ comes first, Inv(G_{P*}) second, and $(G_{P*})_<$ last. One can easily show that A satisfies the hypotheses of Theorem 3.2. That is, the blocks for $(G_{P*})_<$ and $(G_{P*})_>$ are nilpotent, and the reordered matrix is lower block diagonal. Hence, as changing bases preserves shift equivalence, we have computed a simpler representative of $[f_{P*}]_\sigma$.

4.3 Phase III: Finding a Subshift Semi-conjugate to f

Once we have the map f_{P*} on relative homology, we find in this third phase an appropriate subshift of finite type that is semi-conjugate to f. This phase is probably the most difficult, both in terms of the theory behind it, and often the computational work involved. The main theoretical tool we use in this phase is the Lefschetz number (see Definition 2.20). The crucial result is the following corollary to the Lefschetz fixed point theorem (Theorem 2.21).

Corollary 4.2. *Given $N \subseteq X$ which is the union of disjoint compact sets $N_1, \ldots, N_k$, let $S = Inv(N, f)$ and $S' = Inv(N_1, f|_{N_k} \circ \cdots \circ f|_{N_1}) \subseteq S$. Then if*

$$L(S', f|_{N_k} \circ \cdots \circ f|_{N_1}) \neq 0, \tag{31}$$

then $f|_{N_k} \circ \cdots \circ f|_{N_1}$ contains a fixed point in S' that corresponds to a period k point under $f|_S$ whose orbit travels through the regions $N_1, \ldots, N_k$ in order.

From this corollary, we can prove a theorem that allows us to find a semi-conjugacy from a subshift to f. This result from [DFTn07] makes this phase of the computation possible.

Theorem 4.3 (Semi-conjugacy of subshift by Lefschetz). *Let $N \subseteq X$ be the union of disjoint compact sets $N_1, \ldots, N_k$, with $S := Inv(N, f)$. Let $G = (\{1, \ldots, k\}, E)$ be a directed graph such that every edge is in a strongly connected component, and for every cycle $\gamma = a_1, \ldots, a_m$, the corresponding Lefschetz number satisfies*

$$L(Inv(N_{a_1}, f_\gamma), f_\gamma) \neq 0, \tag{32}$$

where $f|_\gamma = f|_{N_{a_m}} \circ \cdots \circ f|_{N_{a_1}}$. Then the itinerary map $\rho : S \to X_G$ is a semi-conjugacy between $f|_{\hat{S}}$ and (X_G, σ_G), where $\hat{S} = \rho^{-1}(X_G)$.

Proof. Let P be the set of periodic points of X_G. Then since all edges of G are in strongly-connected components, we have that X_G is the closure of P; that is, $X_G = \overline{P}$. By Corollary 4.2, for any periodic orbit $\mathbf{s} \in X_G$, there exists a corresponding periodic orbit in $\rho^{-1}(\mathbf{s})$. Then $S' := \overline{\rho^{-1}(P)}$ must be a compact subset of the compact set $S := Inv(N, f)$. Since ρ is continuous and S' is compact, ρ must map S' onto X_G. Finally, since $S' \subseteq \hat{S}$ and $\rho(\hat{S}) \subseteq X_G$, ρ is a semi-conjugacy on $\hat{S}$. □

The only difficulty that remains is finding the directed graph G which satisfies the Lefschetz condition in Theorem 4.3 above, while giving us as much topological entropy as possible. We now show how to construct such a G from f_{P*}.

To simplify the computations, we make an assumption: *assume f_{P*} is trivial for all but one level of homology k.* The procedure would have to be generalized slightly if this is not the case, but in most examples, particularly for Hénon, this assumption is valid.

We now describe the actual computation. The first step is to compute an "upper bound" subshift by taking G_{P*} from the previous section and contracting the generators of each connected region of I to a single vertex. The resulting graph H corresponds to a subshift of finite type which will be semi-conjugate to f if every cycle of H has a nonzero Lefschetz number.

It would seem that we may be done, in light of Theorem 4.3, but there are two potential problems with this step. First, in the case that H has positive topological entropy, which is the case we are interested in, there are infinitely many cycles in H, and thus infinitely many Lefschetz number computations. Secondly, some cycles may have a Lefschetz number of zero, thus leaving us unable to prove that (X_H, σ_H) is semi-conjugate to f.

To solve these problems, we make use of two fairly complicated algorithms. The first attempts to reduce the infinite list of Lefschetz computations down to

a finite list using group theory, and the second copes with the cycles with zero Lefschetz number by removing edges from H. There is a lot of interesting math and computer science embedded in these algorithms, and the interested reader should see [DFTn07] for more details.

4.4 Phase I: Approximating Maximal Symbolic Dynamics

The goal of this phase is to produce a box collection whose index pair captures as much of the complicated dynamics of f as possible. Using topological entropy as the measure of our success in doing so, we can think of this as finding a box collection that leads to a subshift with the highest possible topological entropy, namely $h(f)$. Unfortunately, it may not be possible to achieve $h(f)$ if f is not uniformly hyperbolic (see Section 5). Moreover, the running times for the last two phases of the method, which are described in the two preceding subsections, are often exponential in the grid resolution. For these reasons, we amend our goal to finding maximal symbolic dynamics for a given grid resolution. We will later vary the grid resolution within the limits imposed by the computation times.

The following definition will make the discussion clearer.

Definition 4.4 (Computed bound on topological entropy). *Given a box collection $\mathcal{S} \subseteq \mathcal{G}$, let* subshift$(S)$ *denote the symbol system obtained by running the last two phases of the algorithm on $\mathcal{S}$. Then the function*

$$h_{alg}(\mathcal{S}) := h(\text{subshift}(\mathcal{S})) \tag{33}$$

is the topological entropy bound we get from $\mathcal{S}$.

Note that since our algorithms are deterministic, h_{alg} is well-defined. With this framework, we wish to find $\mathcal{S}$ such that

$$\mathcal{S} \in \text{argmax}_{\mathcal{W} \subseteq \mathcal{G}} \{h_{\text{alg}}(\mathcal{W})\}. \tag{34}$$

Thus, we must solve the above maximization problem, but since there on the order of $2^{2^{nr}}$ such box sets $\mathcal{W}$ if $X \subseteq \mathbb{R}^n$ (or more precisely, $2^{2^{dr}}$, where d is the Hausdorff dimension of the invariant set), this maximization problem is computationally infeasible for high resolutions.

While there are many analytical tools for finding maxima of certain type of functions, these are useless since we have practically no control over the behavior of h_{alg}; the value $h_{\text{alg}}(\mathcal{S})$ depends on the rather complicated procedure outlined in sections 4.2 and 4.3. Therefore, it is useful to think of this maximization as a search over a state space, which allows us to use techniques from the field of Artificial Intelligence. By using these techniques, however, we will have to settle with a potentially suboptimal set $\mathcal{S}$, although we hope that $\mathcal{S}$ will be very close to optimal.

With these ideas in mind, we present below three algorithms for producing box collections. The first is analogous to a greedy algorithm, and builds $\mathcal{S}$ by

adding periodic points of low period. The second approach also uses periodic points, but looks at different combinations of such orbits. Lastly, the third algorithm merely takes the entire invariant set of $\mathcal{G}$, under the assumption that this set is not connected.

4.4.1 Greedy Approximation

The first algorithm we consider uses the heuristic that topological entropy is higher for systems with faster mixing. Thus, we look for periodic points of low periods, and try to find short connections between them. Specifically, we find all box candidates for periodic points (a box whose image contains itself does not necessarily contain a fixed point) up to a fixed period K, and then compute connections between all pairs of these candidates, adding the connections if they are not "too close" to the set so far. This procedure is given more precisely as Algorithm 3.

$\mathcal{S} \leftarrow \emptyset$
for $k = 1 \dots K$ **do**
  $\mathcal{S} \leftarrow \mathcal{S} \cup \{b \mid b \in \mathcal{F}^n(b)\}$
end for
for $i, j \in \mathcal{S}$ **do**
  $\mathcal{W} \leftarrow \mathcal{G} \setminus o(o(\mathcal{S}))$
  $\mathcal{S} \leftarrow \mathcal{S} \cup \{\text{shortest path from } i \text{ to } j \text{ in } \mathcal{F}|_{\mathcal{W}}\}$
end for

Algorithm 3: Greedy Algorithm

The reason for keeping a separation (of two box widths, in this case) is that in order to find a semi-conjugacy, we need to first obtain disjoint compact subsets of the phase space (see Theorem 4.3). If we add too many boxes to our set, the box invariant set will be too connected, and thus we will not be able to find a semi-conjugacy. For more on this algorithm and its application to the classical Hénon map, see [DFTn07].

4.4.2 Breadth-First Search

This second algorithm is in a way a generalization of the first. Using a similar heuristic to the greedy approach, we also compute low periodic points up to some fixed period K. Instead of including all of them in $\mathcal{S}$, however, we try connecting different combinations of periodic orbits together, to make many different sets. To navigate through the possibilities, we use breadth-first search.

Let $\mathcal{O}_1, \dots, \mathcal{O}_n$ be collections of boxes, each of which corresponds to a periodic orbit of period at most K. To generate these sets $\mathcal{O}_i$ we take periodic candidates of a period p, find cycles of length p through those boxes, and and then grow an box isolated invariant set from these using Algorithm 1. Once we have "grown" a periodic orbit $\mathcal{O}_i$ in this way (which in general will have many

more than p boxes), we remove $\mathcal{O}_i$ from the list of candidates and continue until there are no candidates left.

Once we have all the periodic orbits $\mathcal{O}_1, \ldots, \mathcal{O}_n$, we compute pairwise connections $\mathcal{C}_{ij}$ between $\mathcal{O}_i$ and $\mathcal{O}_j$, again using shortest paths, and let $\mathcal{S}_{ij} = \mathcal{O}_i \cup \mathcal{C}_{ij} \cup \mathcal{O}_j$. Conceptually, this set $\mathcal{S}_{ij}$ corresponds to a simple horseshoe-like system, consiting of two periodic orbits and connections between them. This breadth-first search algorithm is also called the Baby Horseshoe Method because of its use of these small sets.

Finally, using the notation $[n] := \{1, \ldots, n\}$, let $A \subseteq [n]$ and define

$$\mathcal{S}_A := \bigcup_{\{i,j \in A \mid i<j\}} \mathcal{S}_{ij} \tag{35}$$

$$h(A) := h\left(\text{subshift}(S_A)\right), \tag{36}$$

where the subshift function is as defined in Definition 4.4.

With the above setup, we simply maximize $h(A)$ over all $A \subseteq [n]$. While this can be done using brute-force search, some convenient pruning assumptions can make the search much more efficient:

1. **Unimodality of h along chains in the subset lattice of $[n]$**
   More precisely, we assume that if $h(A) < h(B)$ for some $B \subset A$, then $h(C) \leq h(A)$ for all $C \supseteq A$. In other words, we assume that if adding $A \backslash B$ to B decreases entropy, then adding more orbits will only decrease the entropy more. This assumption is based on observation, and seems to be true of any chain $S_1 \subset S_2 \cdots \subset S_n$ in the boolean lattice of box collections. The most likely explanation for this phenomenon is that symbol regions tend to glue together as more is added to the set; this gluing often increases the complexity of the region's homology, making transitions through the region harder to prove using Corollary 4.2.

2. **Sets that do not increase entropy can be ignored**
   We assume that if $B \subset A \subseteq [n]$ and $h(B) = h(A)$, then $h(B \cup C) \geq h(A \cup C)$ for all $C \subseteq [n]$. In other words, if $A \setminus B$ did not increase the entropy of B, then either we are in the above case, or $A \setminus B$ will never contribute to the topological entropy of *any* set.

With these assumptions, which can be thought of as heuristics, although they have never proven false in practice, we can use breadth-first search on the Boolean lattice of subsets of $[n]$, pruning the search tree according to the above rules whenever possible. This leads to Algorithm 4.

If the two assumptions above are valid, the Baby Horseshoe Method produces strictly better results than the greedy approach from the previous section, since the greedy approach corresponds to taking $A = [n]$ in Algorithm 4. In fact, this approach often does significantly better, since it can come closer to the "breaking point", where adding more to the set $\mathcal{S}$ actually decreases the topological entropy bound. The main drawback, however, is that Algorithm 4 is more computationally intensive than Algorithm 3.

$C_1 \leftarrow \{\{i\} \mid i \in [n]\}$
for $k = 2 \ldots n$ **do**
  for $A \subseteq [n]$, $|A| = k$ **do**
    $C_A \leftarrow \{B \in C_{k-1} \mid B \subset A\}$
    if $|C_A| = k$ and $h(A) > h(B)$ for all $B \in C_A$ **then**
      $C_k \leftarrow C_k \cup \{A\}$
    end if
  end for
end for

Algorithm 4: Baby Horseshoe Method

4.4.3 Maximal Invariant Set

The final method of producing a box set $\mathcal{S}$ is to just take $\mathcal{S} = \mathrm{Inv}(\mathcal{F})$. In words, we merely take the box invariant set of the entire grid $\mathcal{G}$ as our set. In many situations, such as the classical parameters for Hénon, this box set is connected. In these cases, Phase II and Phase III of our algorithm yield a trivial semi-conjugacy which gives a lower bound of 0 for the topological entropy. If the box invariant set can be separated into non-neighboring sets of boxes, however, this approach tends to work remarkably well. In fact, this approach is precisely what we need for hyperbolic maps, which we discuss in the next section.

5 Applications to Hyperbolicity

5.1 Lower Bounds for Hyperbolic Plateaus of Hénon

We now apply the methods outlined in Section 4 to the Hénon maps. Specifically, we focus on parameter values (a, b) whose corresponding map $f_{a,b}$ has a special structure known as hyperbolicity. This structure can be thought of as a generalization of the structure of the Smale horseshoe, namely that there are invariant directions, and there is uniform contraction and expansion in the stable and unstable directions, respectively. Some useful properties of hyperbolic systems are discussed below, but for more details see [Rob95] and [GH90].

Automated methods for proving hyperbolicity have only been introduced recently, by Suzanne Hruska [Hru06] and Zin Arai [Araar]. We focus here on the work of Zin Arai for the Hénon family in which he shows that the regions in Figure 1 are hyperbolic.

Arai uses a somewhat indirect technique to prove hyperbolicity which allows for more efficient computations than Hruska. As a consequence, however, his technique does not guarantee that the non-wandering is not just a finite collection of periodic orbits, or even that it is nonempty. Specifically, Arai's technique does not give any information about the topological entropy of the regions in question. This is one motivation for applying our automated method to the plateaus computed by Arai.

Another motivation is that topological entropy is constant on the hyperbolic

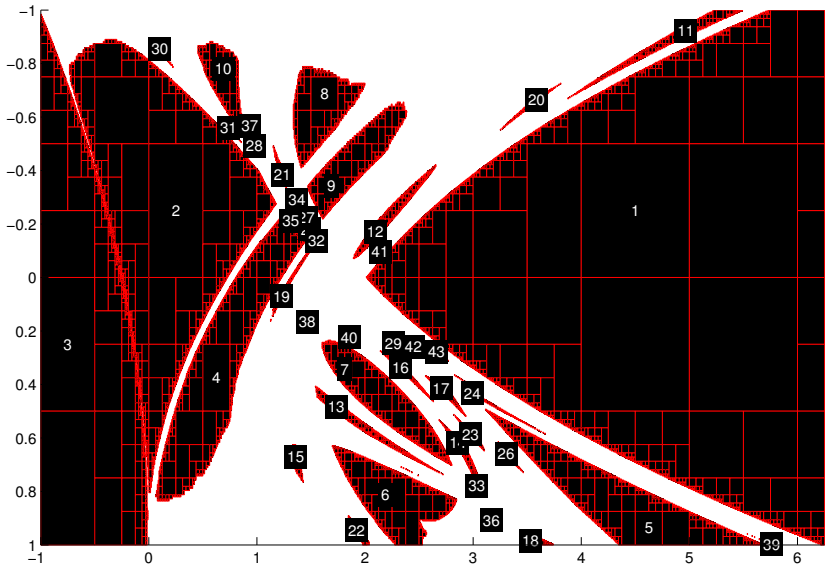

Figure 1: Hyperbolic plateaus for Hénon, as computed by Zin Arai, with a on the horizontal axis and b on the vertical axis. The plateaus are labeled for reference, and each label is centered over the parameter values we use for its plateau.

plateaus. This follows from the fact that hyperbolic maps are structurally stable (see Chapter 9.9 of [Rob95]), so all maps in the same hyperbolic plateau are conjugate. Thus, by Theorem 2.11, the topological entropy for these maps is the same. By computing a lower bound for the topological entropy of $f_{a,b}$ for some parameter point (a, b) in a hyperbolic plateau P, we therefore have the same lower bound on every point $(a', b') \in P$. In some sense, this allows us to get a lot of information about topological entropy as a function of the parameter space "for free" by computing lower bounds for a small number of points.

Computing lower bounds for the topological entropy of the plateaus is a very straightforward application of our technique outlined in section 4. Specifically, since we are dealing with parameters for which Hénon is hyperbolic, the maximal invariant set is guaranteed to be disconnected (see [Mil88]), so we can apply the "maximal invariant set" method from Section 4.4.3. Figure 2 shows our results. Also, see Appendix A for index pairs and subshifts for the plateaus with nonzero entropy bounds.

Note that the values in Figure 2 are not necessarily the true entropy values for the plateaus; they are merely lower bounds. Since we are computing these bounds for hyperbolic parameter values, however, we know that the system is conjugate to some subshift of finite type. Thus, if the entropy lower bound that we compute for a given map levels off as the grid resolution increases, we have strong evidence that the lower bound is tight. In other words, we would

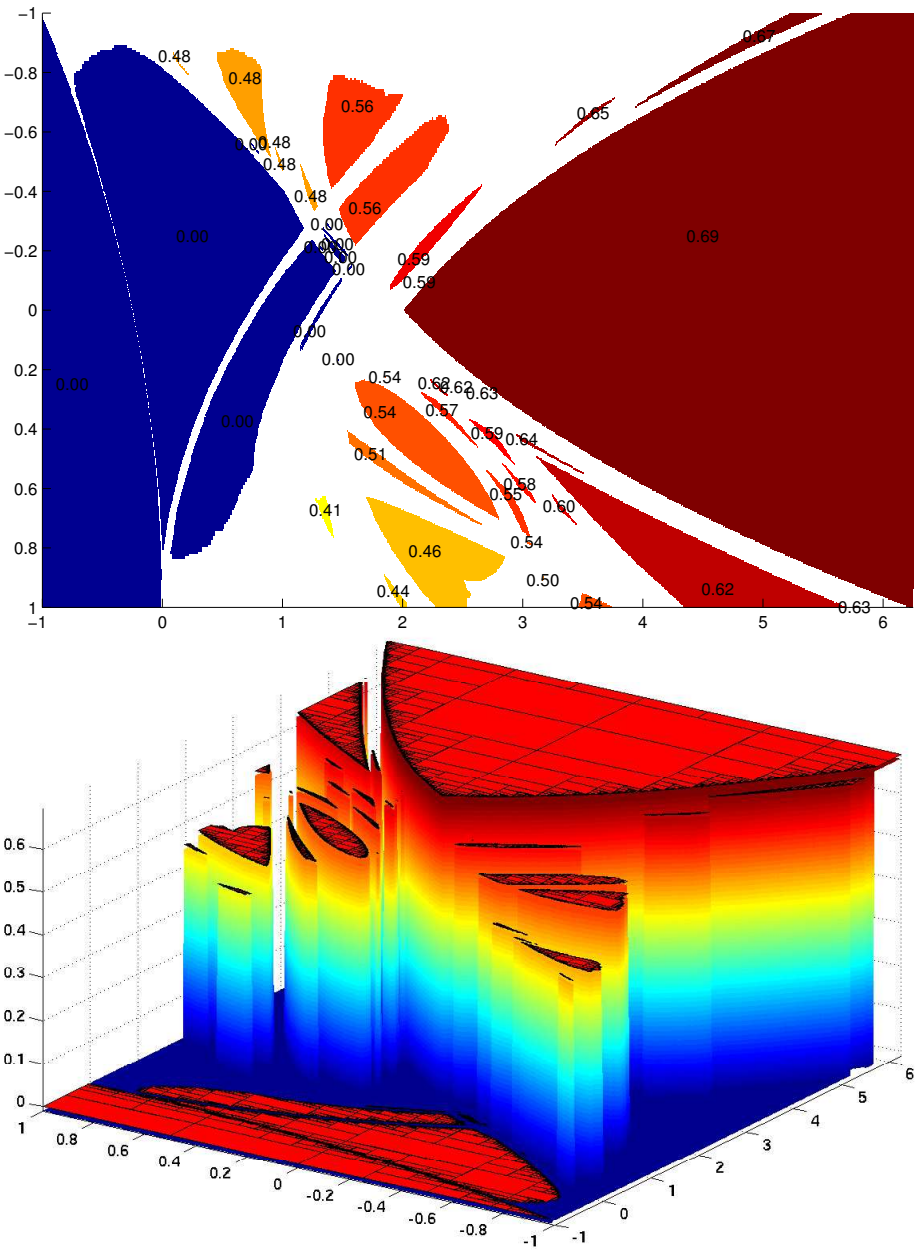

Figure 2: Rigorous lower bounds for topological entropy for the hyperbolic plateaus labeled 1 through 43 in Figure 1.

have evidence that the itinerary map ρ is a conjugacy rather than just a semi-conjugacy, and that the entropy bound that we computed is the true value.

To actually prove that the itinerary map ρ is a conjugacy, we would need to show that ρ is injective in addition to being a semi-conjugacy (see Definition 2.9). To prove this, we would need to show that the map is hyperbolic in a manner compatible with our index pair or Markov partition. For example, it might be enough to show that each region of the index pair had an unstable manifold that mapped across the region and into the exit set without folding, and a similar condition for the stable direction. One might be able to automate this proof by using a technique similar to that of Arai or Hruska.

The plots on the right-hand side in Appendix A show how the topological entropy lower bound $h_{\text{alg}}(f)$ computed by our algorithm varies with the grid resolution. Rather than just varying r for $\mathcal{G}^{(r)}$ directly, we vary the bounds of W (see Definition 2.22) as well, since taking W twice as large for $\mathcal{G}^{(r)}$ is the same as $\mathcal{G}^{(r+1)}$, provided that the original W covered the invariant set of f. In this way, we can "continuously" vary the resolution of the grid.

The plots in Appendix A reveal some unexpected behavior of the algorithm, and offer insight into the nature of maximal symbolic dynamics as a function of the grid resolution. One observation is that most of the plateaus have plots with spikes of positive entropy separated by periods of zero entropy, and some of these spikes have no perceivable pattern, such as for plateau 18 or 33. Moreover, some plots (e.g. for plateaus 7, 8, 9) have the highest entropy lower bound occurring at the first grid resolution with nonzero entropy.

These observations seem to contradict the intuitive notion that the maximal topological entropy value for $\mathcal{G}^{(r)}$ should increase with r, since the grid is becoming more refined. In fact, one can show that a box index pair for some $\mathcal{G}^{(r)}$ is also an index pair for $\mathcal{G}^{(r+1)}$, so the maximal topological entropy for a grid cannot have a net decrease with r. Unfortunately, this "ideal" behavior is rare in practice, with plateau 5 being the only good example. This shows that our algorithm is sometimes significantly suboptimal for a given grid, and this is part of the reason we look at many grids for each plateau.

Assuming the lower bounds presented are at least close to the true values, Figure 2 suggests some sort of monotonicity of entropy as the parameters are varied. Specifically, it seems that entropy is roughly monotone along lines that are perpendicular to the boundary of the maximal entropy plateau (plateau 1). Also of interest is the progress toward finding the boundary of zero entropy for Hénon.

5.2 Lower Bounds for the Area-Preserving Hénon Maps

When $b = -1$, the Hénon maps are area-preserving and orientation-preserving. This case has been well-studied in the Physics literature especially; we focus here on the work of Davis, MacKay, and Sannami [DMS91].

For three different values of a, Davis, et al. give symbolic dynamics which they conjecture to be conjugate to Hénon at those parameters. Zin Arai also computed one-dimensional hyperbolic plateaus for when $b = -1$, so using the

same technique as with the 2-dimensional plateaus, we can attempt to verify that the symbol graphs given in [DMS91] are semi-conjugate to Hénon with the appropriate parameters.

For the value $a = 5.4$, Davis, et al. conjectured that f_a is conjugate to the subshift corresponding to the following transition matrix T_{DMS}, which has topological entropy $h(T_{\text{DMS}}) = 0.6774$.

$$T_{\text{DMS}} = \begin{array}{c} \\ A \\ B \\ C \\ D \\ E \\ F \\ G \\ H \end{array} \begin{array}{c} \begin{array}{cccccccc} A & B & C & D & E & F & G & H \end{array} \\ \begin{bmatrix} 1 & 1 & 0 & 0 & 0 & 0 & 0 & 0 \\ 0 & 0 & 0 & 1 & 1 & 0 & 1 & 0 \\ 0 & 0 & 0 & 1 & 0 & 1 & 0 & 1 \\ 0 & 0 & 0 & 0 & 1 & 0 & 0 & 0 \\ 1 & 0 & 0 & 0 & 0 & 0 & 0 & 0 \\ 0 & 0 & 1 & 1 & 0 & 0 & 0 & 0 \\ 0 & 0 & 1 & 0 & 0 & 1 & 0 & 1 \\ 0 & 0 & 0 & 1 & 0 & 1 & 0 & 1 \end{bmatrix} \end{array} \tag{37}$$

Using our technique, we obtain a 42×42 symbol matrix T_{alg} which is semi-conjugate to $f_{5.4}$. The topological entropy of this matrix is the same value, $h(T_{\text{alg}}) = 0.6774$, thus showing that the value for topological entropy (implicitly) conjectured by Davis, et al. is in fact a lower bound.

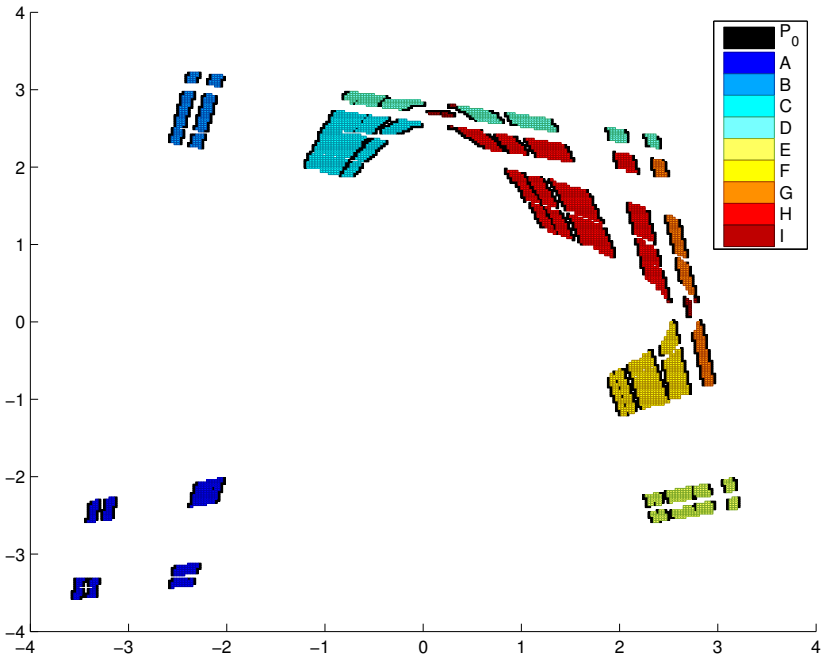

Figure 3: Index pair for $a = 5.4$ and $b = -1$, with regions colored to indicate the symbols for the smaller shift-equivalent symbol system.

The fact that $h(T_{\text{DMS}}) = h(T_{\text{alg}})$ suggests that the subshifts given by T_{DMS} and T_{alg} might be conjugate. In fact, by repeatly applying Theorem 3.1 for the right choice of vertices, we obtain a strong shift equivalence between T_{DMS} and T_{alg}, which shows that the corresponding subshifts are indeed conjugate. Moreover, the contracted vertices can be chosen so that we obtain the same Markov partition that was conjectured by Davis, et al. This is shown in Figure 3, with the colored regions labeled so as to match the labels in (37) above.

Davis, et al. also looked at two other parameter values for Hénon, namely $a = 5.59$ and $a = 5.65$. Unfortunately, our method was not able to compute lower bounds that match the topological entropy of the subshifts matrices given in [DMS91]. The plots of entropy verses resolution in Appendix B for these two parameter values seem to level off slightly, but it is likely that after more computations, our method will be produce bounds that match the results of Davis, et al.

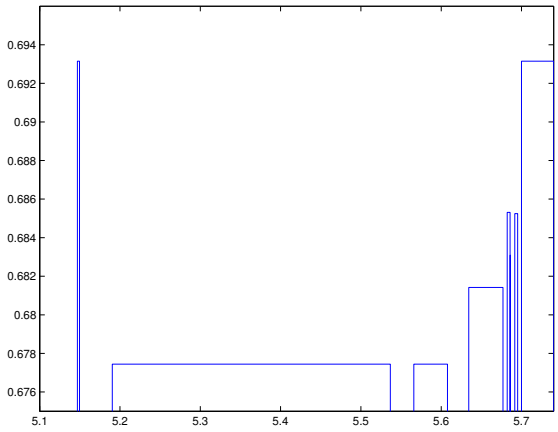

Figure 4: Rigorous lower bounds for topological entropy of the area-preserving Hénon maps, where $b = -1$. The plot shows $h_{\text{alg}}(f_a)$ plotted against a.

In addition to the three area-preserving parameter values studied by Davis, Mackay and Sannami, we also focus on five other values, which all together correspond to the last eight area-preserving intervals computed by Arai:

$$\begin{array}{rcll} 5.1483 & \in & [5.1470 & 5.1497] \\ 5.4000 & \in & [5.1904 & 5.5366] \\ 5.5900 & \in & [5.5659 & 5.6078] \\ 5.6500 & \in & [5.6343 & 5.6769] \\ 5.6839 & \in & [5.6821 & 5.6858] \\ 5.6859 & \in & [5.6859 & 5.6860] \\ 5.6934 & \in & [5.6917 & 5.6952] \\ 5.8499 & \in & [5.7000 & \infty), \end{array}$$

where the a values on the left are the representatives we use for each interval. Figure 4 shows a plot of the resulting lower bounds for topological entropy we

compute for these intervals. Particularly interesting is the entropy of log(2) obtained in the first interval, since this interval is not part of the maximal entropy plateau. Aside from this interval, the topological entropy seems to be monotone increasing with a.

6 Acknowledgements

The author would like to thank John Smillie for all of his guidance, candid advice, and patience throughout the past year. He also thanks Zin Arai for sending his useful data, and Sarah Day for giving many helpful comments.

References

[Araar] Zin Arai, *On hyperbolic plateaus of the hénon maps*, Experimental Mathmatics, to appear.

[cho] *Computational Homology Project (CHomP)*, (http://www.math.gatech.edu/∽chomp/).

[Cse99] Tibor Csendes (ed.), *INTLAB - INTerval LABoratory*, Dordrecht, Springer, 1999, Proceedings of the International Symposium on Scientific Computing, Computer Arithmetic and Validated Numerics. Selected papers from the symposium (SCAN-98) held in Budapest, September 22–25, 1998, Reprinted in *Developments in reliable computing* [213–357, Kluwer Acad. Publ., Dordrecht, 1999], Reliab. Comput. **5** (1999), no. 3. MR MR1743193 (2001b:65007b)

[DFJ01] Michael Dellnitz, Gary Froyland, and Oliver Junge, *The algorithms behind GAIO-set oriented numerical methods for dynamical systems*, Ergodic theory, analysis, and efficient simulation of dynamical systems, Springer, Berlin, 2001, pp. 145–174, 805–807. MR 2002k:65217

[DFTn07] Sarah Day, Rafael Frongillo, and Rodrigo Treviño, *Algorithms for rigorous entropy bounds and symbolic dynamics*, preprint, 2007.

[DMS91] M. J. Davis, R. S. MacKay, and A. Sannami, *Markov shifts in the Hénon family*, Phys. D **52** (1991), no. 2-3, 171–178. MR MR1128987 (92g:58099)

[Eve79] Shimon Even, *Graph algorithms*, Computer Science Press Inc., Woodland Hills, Calif., 1979, Computer Software Engineering Series. MR MR540205 (82e:68066)

[GH90] John Guckenheimer and Philip Holmes, *Nonlinear oscillations, dynamical systems, and bifurcations of vector fields*, Applied Mathematical Sciences, vol. 42, Springer-Verlag, New York, 1990, Revised and corrected reprint of the 1983 original. MR MR1139515 (93e:58046)

[Hru06] Suzanne Lynch Hruska, *A numerical method for constructing the hyperbolic structure of complex Hénon mappings*, Found. Comput. Math. **6** (2006), no. 4, 427–455. MR MR2271215

[LM95] Douglas Lind and Brian Marcus, *An introduction to symbolic dynamics and coding*, Cambridge University Press, Cambridge, 1995.

[Mil88] John Milnor, *Nonexpansive Hénon maps*, Adv. in Math. **69** (1988), no. 1, 109–114. MR MR937319 (89g:58174)

[MM02] Konstantin Mischaikow and Marian Mrozek, *Conley index*, Handbook of Dynamical Systems, Elsevier, Berlin, 2002, pp. 393–460.

[Pil98] P. Pilarczyk, *Homology computation-software and examples*, Jagiellonian University, 1998, (http://www.im.uj.edu.pl/~pilarczy/homology.htm).

[Rob95] Clark Robinson, *Dynamical systems*, Studies in Advanced Mathematics, CRC Press, Boca Raton, FL, 1995, Stability, symbolic dynamics, and chaos. MR MR1396532 (97e:58064)

[Szy97] Andrzej Szymczak, *A combinatorial procedure for finding isolating neighbourhoods and index pairs*, Proc. Roy. Soc. Edinburgh Sect. A **127** (1997), no. 5, 1075–1088. MR MR1475647 (98i:58151)

[Wil73] R. F. Williams, *Classification of subshifts of finite type*, Recent advances in topological dynamics (Proc. Conf. Topological Dynamics, Yale Univ., New Haven, Conn., 1972; in honor of Gustav Arnold Hedlund), Springer, Berlin, 1973, pp. 281–285. Lecture Notes in Math., Vol. 318. MR MR0391060 (52 #11882)

A Index Pairs for Hyperbolic Plateaus

1

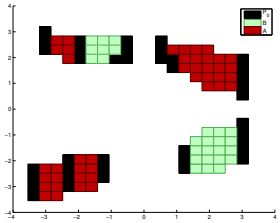

	A	B
A	**1**	**1**
B	**1**	**1**

a=4.5000 b=−0.2500

$h_{\mathrm{alg}}(f_{a,b}) = 0.6931$

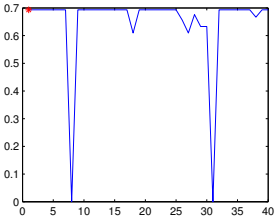

5

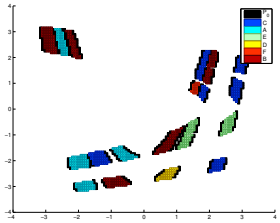

	A	B	C	D	E	F
A	0	**1**	0	0	0	0
B	**1**	0	**1**	0	**1**	0
C	0	0	**1**	**1**	**1**	**1**
D	**1**	0	0	0	0	0
E	0	0	0	**1**	**1**	0
F	**1**	0	0	0	0	0

a=4.6250 b=0.9375

$h_{\mathrm{alg}}(f_{a,b}) = 0.6292$

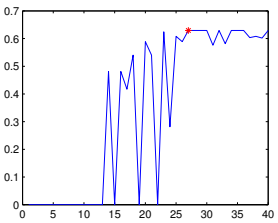

6

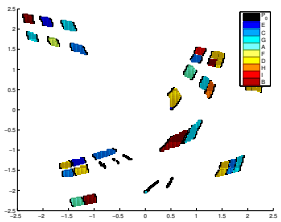

$$\begin{array}{c} \\ A \\ B \\ C \\ D \\ E \\ F \\ G \\ H \\ I \end{array} \begin{array}{c} \begin{array}{ccccccccc} A & B & C & D & E & F & G & H & I \end{array} \\ \left[\begin{array}{ccccccccc} 0 & \mathbf{1} & 0 & 0 & 0 & 0 & 0 & 0 & 0 \\ 0 & 0 & \mathbf{1} & \mathbf{1} & 0 & \mathbf{1} & 0 & 0 & 0 \\ 0 & 0 & 0 & 0 & \mathbf{1} & 0 & \mathbf{1} & 0 & 0 \\ 0 & 0 & 0 & \mathbf{1} & 0 & 0 & \mathbf{1} & 0 & 0 \\ \mathbf{1} & 0 & 0 & 0 & 0 & 0 & 0 & 0 & 0 \\ 0 & 0 & 0 & 0 & 0 & \mathbf{1} & 0 & \mathbf{1} & \mathbf{1} \\ 0 & 0 & \mathbf{1} & 0 & 0 & 0 & 0 & 0 & 0 \\ 0 & 0 & 0 & 0 & 0 & 0 & 0 & 0 & \mathbf{1} \\ 0 & 0 & 0 & \mathbf{1} & 0 & 0 & 0 & 0 & 0 \end{array}\right] \end{array}$$

a=2.1875 b=0.8125

$h_{\text{alg}}(f_{a,b}) = 0.4651$

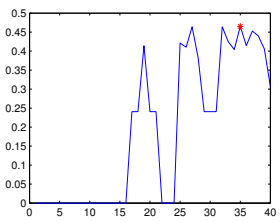

7

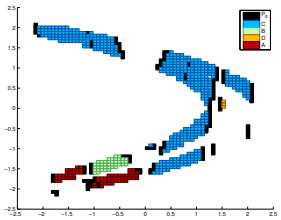

$$\begin{array}{c} \\ A \\ B \\ C \\ D \end{array} \begin{array}{c} \begin{array}{cccc} A & B & C & D \end{array} \\ \left[\begin{array}{cccc} 0 & \mathbf{1} & 0 & \mathbf{1} \\ \mathbf{1} & 0 & 0 & 0 \\ 0 & \mathbf{1} & \mathbf{1} & 0 \\ 0 & 0 & \mathbf{1} & \mathbf{1} \end{array}\right] \end{array}$$

a=1.8125 b=0.3438

$h_{\text{alg}}(f_{a,b}) = 0.5404$

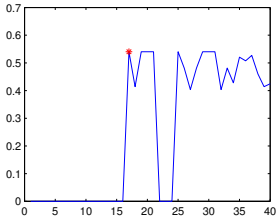

8

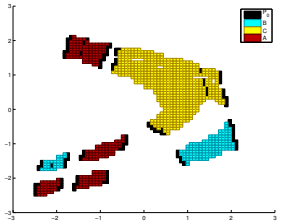

$$\begin{array}{c} \\ A \\ B \\ C \end{array} \begin{array}{c} \begin{array}{ccc} A & B & C \end{array} \\ \left[\begin{array}{ccc} \mathbf{1} & 0 & \mathbf{1} \\ \mathbf{1} & \mathbf{1} & 0 \\ 0 & \mathbf{1} & 0 \end{array}\right] \end{array}$$

a=1.6250 b=−0.6875

$h_{\text{alg}}(f_{a,b}) = 0.5624$

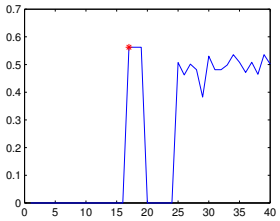

9

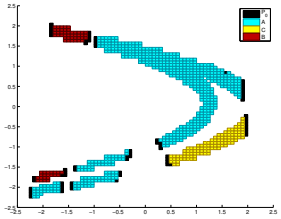

$$\begin{array}{c} \\ A \\ B \\ C \end{array} \begin{array}{c} \begin{array}{ccc} A & B & C \end{array} \\ \left[\begin{array}{ccc} \mathbf{1} & \mathbf{1} & 0 \\ 0 & \mathbf{1} & \mathbf{1} \\ \mathbf{1} & 0 & 0 \end{array}\right] \end{array}$$

a=1.6875 b=−0.3438

$h_{\text{alg}}(f_{a,b}) = 0.5624$

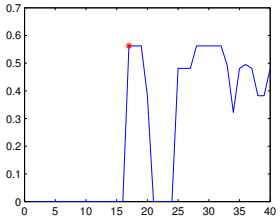

10

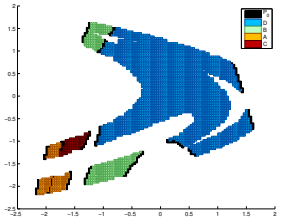

$$\begin{array}{c} \\ A \\ B \\ C \\ D \end{array} \begin{array}{c} \begin{array}{cccc} A & B & C & D \end{array} \\ \left[\begin{array}{cccc} \mathbf{1} & \mathbf{1} & 0 & 0 \\ 0 & 0 & 0 & \mathbf{1} \\ \mathbf{1} & 0 & \mathbf{1} & 0 \\ 0 & 0 & \mathbf{1} & 0 \end{array}\right] \end{array}$$

a=0.6875 b=−0.7812

$h_{\text{alg}}(f_{a,b}) = 0.4812$

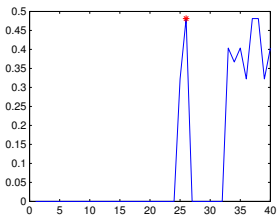

11

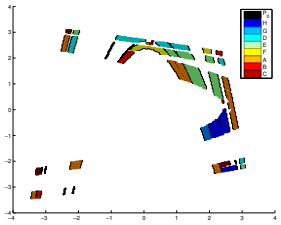

	A	B	C	D	E	F	G	H
A	1	1	0	0	0	1	0	0
B	0	0	0	0	1	0	0	0
C	1	0	0	0	1	1	1	0
D	0	1	0	1	0	0	0	1
E	0	0	0	1	0	0	0	0
F	1	1	0	0	0	0	0	0
G	1	1	0	0	0	0	0	0
H	0	0	1	0	0	0	0	0

a=4.9688 b=−0.9219

$h_{\text{alg}}(f_{a,b}) = 0.6683$

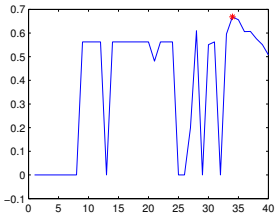

12

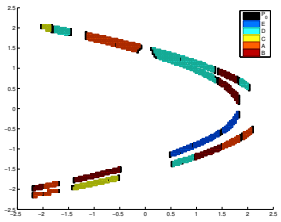

	A	B	C	D	E
A	1	0	1	0	0
B	0	0	0	1	1
C	0	1	0	0	1
D	0	1	0	1	0
E	1	0	0	0	0

a=2.0938 b=−0.1719

$h_{\text{alg}}(f_{a,b}) = 0.5967$

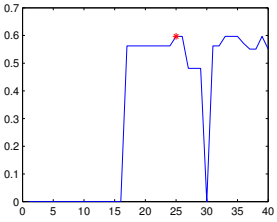

13

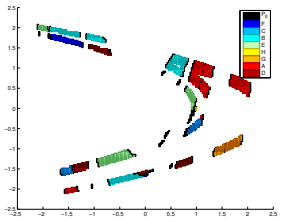

	A	B	C	D	E	F	G	H
A	0	0	0	0	0	1	0	1
B	0	1	0	0	1	1	1	0
C	0	0	0	1	0	0	0	0
D	1	1	0	0	0	0	0	0
E	1	0	0	0	1	0	0	0
F	1	0	0	0	0	0	0	0
G	1	0	0	0	0	0	0	0
H	0	0	1	0	0	0	0	0

a=1.7344 b=0.4844

$h_{\text{alg}}(f_{a,b}) = 0.5134$

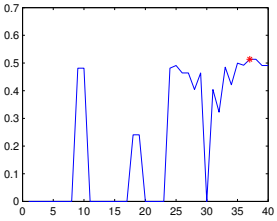

14

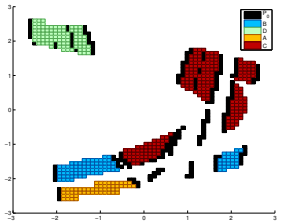

	A	B	C	D
A	0	1	0	0
B	1	0	0	1
C	1	0	1	0
D	0	0	1	1

a=2.8594 b=0.6172

$h_{\text{alg}}(f_{a,b}) = 0.5404$

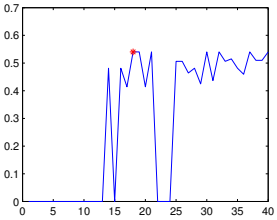

15

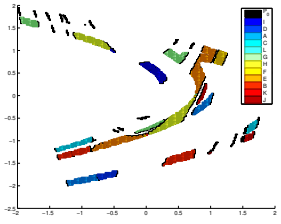

a=1.3594 b=0.6719

$h_{\text{alg}}(f_{a,b}) = 0.4097$

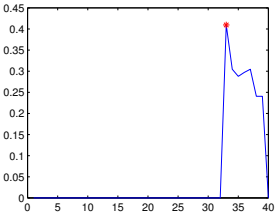

16

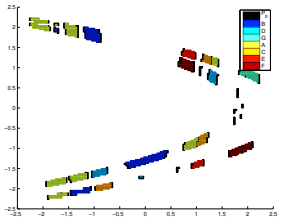

	A	B	C	D	E	F	G
A	1	1	0	1	1	0	0
B	0	1	0	1	0	0	0
C	1	0	0	0	0	1	1
D	0	0	0	0	1	0	0
E	0	0	0	0	0	1	0
F	0	0	1	0	0	0	0
G	0	1	0	0	0	0	0

a=2.3281 b=0.3359

$h_{\text{alg}}(f_{a,b}) = 0.5573$

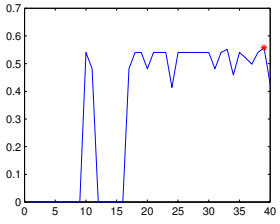

17

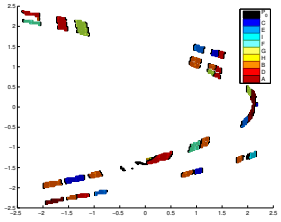

	A	B	C	D	E	F	G	H	I
A	0	0	0	0	0	1	0	0	0
B	0	1	1	0	0	0	1	1	0
C	1	0	0	0	0	0	0	0	0
D	0	0	0	0	1	0	1	0	1
E	0	1	0	1	0	0	0	0	0
F	0	0	0	0	1	0	0	0	0
G	0	0	1	0	0	0	1	0	0
H	0	0	0	1	0	0	0	0	0
I	0	0	1	0	0	0	1	0	0

a=2.7031 b=0.4141

$h_{\text{alg}}(f_{a,b}) = 0.5905$

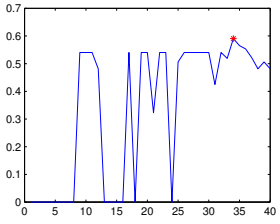

18

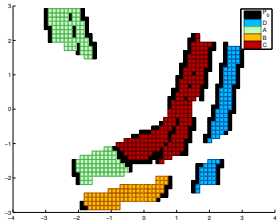

	A	B	C	D
A	1	1	0	0
B	0	0	0	1
C	1	0	1	0
D	0	1	1	0

a=3.5312 b=0.9844

$h_{\text{alg}}(f_{a,b}) = 0.5404$

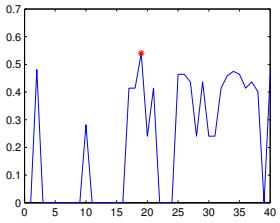

20

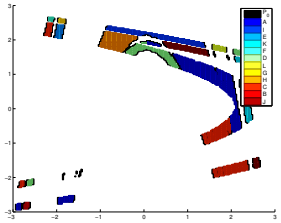

a=3.5859 b=−0.6641

$h_{\text{alg}}(f_{a,b}) = 0.6345$

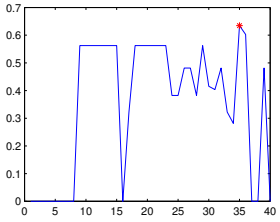

21

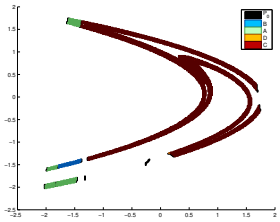

	A	B	C	D
A	1	1	0	0
B	0	0	1	0
C	0	0	1	1
D	1	0	0	0

a=1.2344 b=−0.3828

$h_{\text{alg}}(f_{a,b}) = 0.4812$

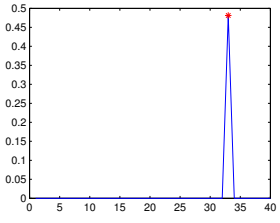

22

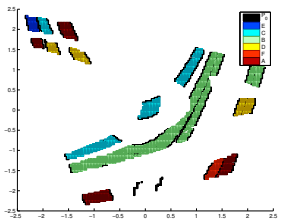

$$\begin{array}{c} \\ A \\ B \\ C \\ D \\ E \\ F \end{array}\begin{array}{c} \begin{array}{cccccc} A & B & C & D & E & F \end{array} \\ \begin{bmatrix} 0 & 0 & \mathbf{1} & 0 & 0 & 0 \\ \mathbf{1} & 0 & 0 & 0 & \mathbf{1} & 0 \\ \mathbf{1} & 0 & 0 & \mathbf{1} & 0 & 0 \\ 0 & \mathbf{1} & 0 & 0 & 0 & 0 \\ 0 & 0 & 0 & 0 & 0 & \mathbf{1} \\ \mathbf{1} & 0 & 0 & 0 & 0 & \mathbf{1} \end{bmatrix} \end{array}$$

a=1.9219 b=0.9453

$h_{\mathrm{alg}}(f_{a,b}) = 0.3822$

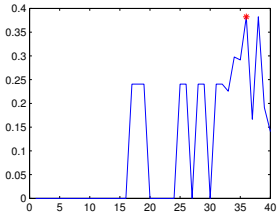

23

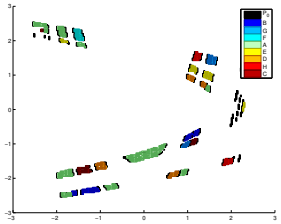

$$\begin{array}{c} \\ A \\ B \\ C \\ D \\ E \\ F \\ G \\ H \end{array}\begin{array}{c} \begin{array}{cccccccc} A & B & C & D & E & F & G & H \end{array} \\ \begin{bmatrix} \mathbf{1} & \mathbf{1} & 0 & \mathbf{1} & \mathbf{1} & 0 & 0 & 0 \\ 0 & \mathbf{1} & 0 & \mathbf{1} & 0 & 0 & 0 & 0 \\ \mathbf{1} & 0 & 0 & 0 & 0 & 0 & 0 & 0 \\ 0 & 0 & 0 & 0 & 0 & 0 & \mathbf{1} & 0 \\ 0 & 0 & 0 & 0 & 0 & \mathbf{1} & 0 & \mathbf{1} \\ 0 & \mathbf{1} & 0 & 0 & 0 & 0 & 0 & 0 \\ 0 & 0 & 0 & 0 & 0 & 0 & 0 & \mathbf{1} \\ 0 & 0 & \mathbf{1} & 0 & \mathbf{1} & 0 & 0 & 0 \end{bmatrix} \end{array}$$

a=2.9766 b=0.5859

$h_{\mathrm{alg}}(f_{a,b}) = 0.5686$

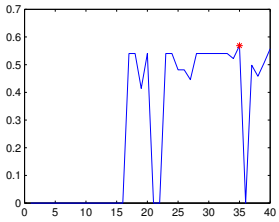

24

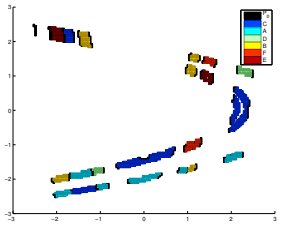

$$\begin{array}{c} \\ A \\ B \\ C \\ D \\ E \\ F \end{array}\begin{array}{c} \begin{array}{cccccc} A & B & C & D & E & F \end{array} \\ \begin{bmatrix} 0 & 0 & \mathbf{1} & 0 & 0 & 0 \\ \mathbf{1} & \mathbf{1} & 0 & 0 & 0 & 0 \\ \mathbf{1} & 0 & 0 & 0 & \mathbf{1} & 0 \\ 0 & \mathbf{1} & 0 & \mathbf{1} & 0 & 0 \\ \mathbf{1} & \mathbf{1} & 0 & 0 & 0 & \mathbf{1} \\ \mathbf{1} & \mathbf{1} & 0 & \mathbf{1} & 0 & 0 \end{bmatrix} \end{array}$$

a=2.9922 b=0.4336

$h_{\mathrm{alg}}(f_{a,b}) = 0.6007$

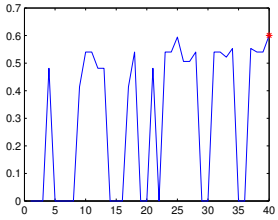

26

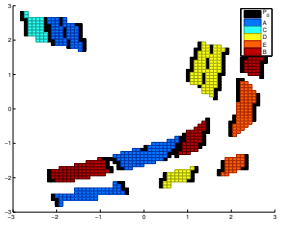

$$\begin{array}{c} \\ A \\ B \\ C \\ D \\ E \end{array}\begin{array}{c} \begin{array}{ccccc} A & B & C & D & E \end{array} \\ \begin{bmatrix} \mathbf{1} & 0 & 0 & \mathbf{1} & 0 \\ \mathbf{1} & 0 & \mathbf{1} & 0 & \mathbf{1} \\ \mathbf{1} & 0 & \mathbf{1} & \mathbf{1} & 0 \\ 0 & 0 & 0 & 0 & \mathbf{1} \\ 0 & \mathbf{1} & 0 & 0 & 0 \end{bmatrix} \end{array}$$

a=3.3047 b=0.6602

$h_{\mathrm{alg}}(f_{a,b}) = 0.5889$

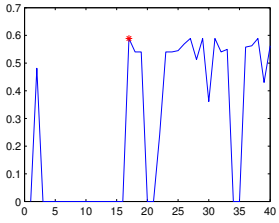

28

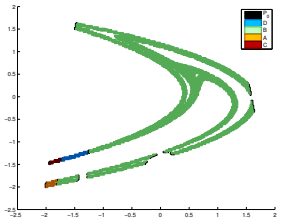

$$\begin{array}{c} \\ A \\ B \\ C \\ D \end{array}\begin{array}{c} \begin{array}{cccc} A & B & C & D \end{array} \\ \begin{bmatrix} 0 & 0 & 0 & \mathbf{1} \\ 0 & \mathbf{1} & \mathbf{1} & 0 \\ \mathbf{1} & 0 & \mathbf{1} & 0 \\ 0 & \mathbf{1} & 0 & 0 \end{bmatrix} \end{array}$$

a=0.9766 b=−0.4922

$h_{\mathrm{alg}}(f_{a,b}) = 0.4812$

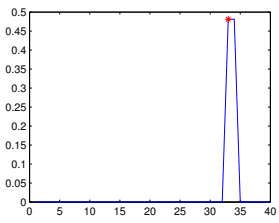

29

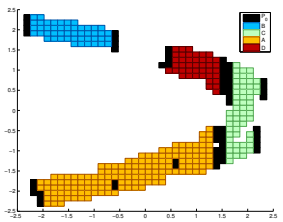

	A	B	C	D
A	**1**	**1**	0	0
B	0	0	**1**	0
C	**1**	**1**	0	**1**
D	**1**	0	0	**1**

a=2.2617 b=0.2461

$h_{\text{alg}}(f_{a,b}) = 0.6242$

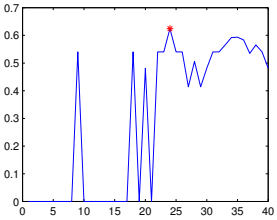

33

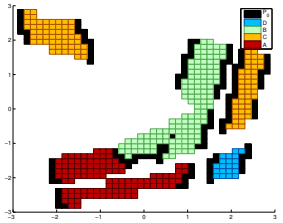

	A	B	C	D
A	**1**	0	0	**1**
B	**1**	**1**	0	0
C	0	**1**	0	**1**
D	0	0	**1**	0

a=3.0352 b=0.7793

$h_{\text{alg}}(f_{a,b}) = 0.5404$

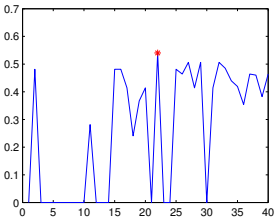

B Index Pairs for Area-Preserving Case

1

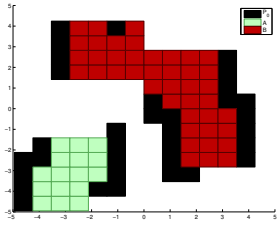

	A	B
A	**1**	**1**
B	**1**	**1**

a=5.1483 b=−1.0000

$h_{\text{alg}}(f_{a,b}) = 0.6931$

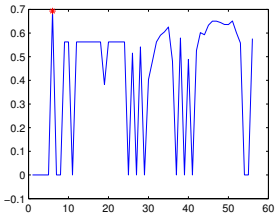

2

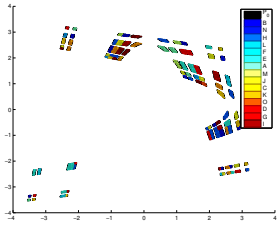

a=5.4000 b=−1.0000

$h_{\text{alg}}(f_{a,b}) = 0.6774$

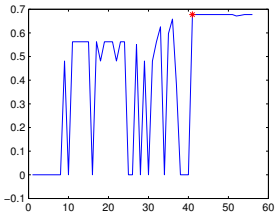

3

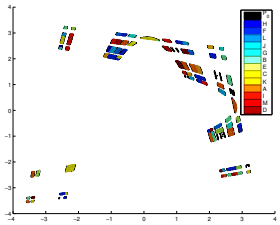

a=5.5900 b=−1.0000

$h_{\text{alg}}(f_{a,b}) = 0.6774$

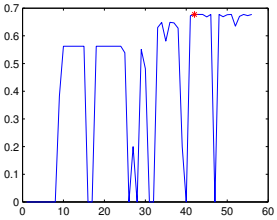

4

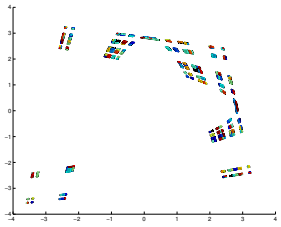

a=5.6500 b=−1.0000

$h_{\text{alg}}(f_{a,b}) = 0.6814$

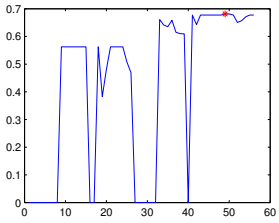

5

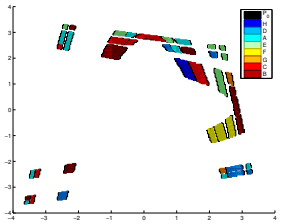

	A	B	C	D	E	F	G	H
A	0	**1**	0	0	0	0	0	0
B	0	0	**1**	0	0	0	0	0
C	**1**	0	**1**	0	0	**1**	0	0
D	0	0	0	0	**1**	0	0	0
E	**1**	0	0	**1**	**1**	0	0	0
F	**1**	0	0	**1**	0	0	**1**	**1**
G	0	0	0	0	**1**	0	0	0
H	**1**	0	0	**1**	**1**	0	**1**	0

a=5.6840 b=−1.0000

$h_{\text{alg}}(f_{a,b}) = 0.6853$

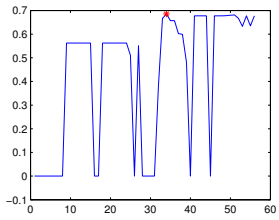

6

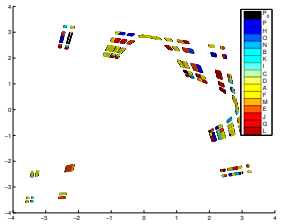

a=5.6860 b=−1.0000

$h_{\text{alg}}(f_{a,b}) = 0.6831$

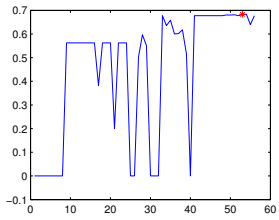

7

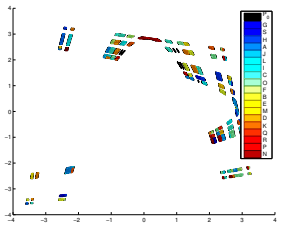

a=5.6934 b=−1.0000

$h_{\text{alg}}(f_{a,b}) = 0.6852$

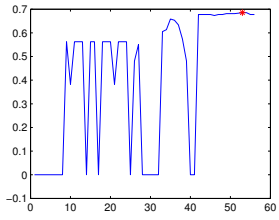

8

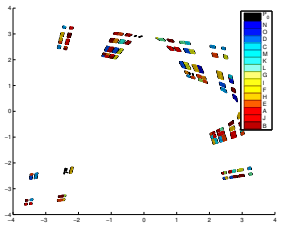

a=5.8500 b=−1.0000

$h_{\text{alg}}(f_{a,b}) = 0.6931$